

# Circuit-based erasure conversion of leakage errors in neutral atoms

Matthew N. H. Chow<sup>‡,1,2,3,\*</sup> Vikas Buchemmavari<sup>‡,2,3,†</sup> Sivaprasad Omanakuttan,<sup>2,3</sup>  
Bethany J. Little,<sup>1</sup> Saurabh Pandey,<sup>1</sup> Ivan H. Deutsch,<sup>2,3</sup> and Yuan-Yu Jau<sup>1,2,3</sup>

<sup>1</sup>*Sandia National Laboratories, Albuquerque, New Mexico 87123, USA*

<sup>2</sup>*Center for Quantum Information and Control (CQuIC),  
University of New Mexico, Albuquerque, NM 87131, USA*

<sup>3</sup>*Department of Physics and Astronomy, University of New Mexico, Albuquerque, NM 87131, USA<sup>‡</sup>*

Leakage out of the computational subspace (predominantly by atom loss) is a major limitation of current state-of-the-art neutral atom quantum computers and a significant challenge for long-term prospects of the platform. We demonstrate proof-of-principle circuit-based conversion of leakage errors to erasure errors in a neutral atom quantum processor via “Leakage Detection Units,” (LDUs) which non-destructively map qubit presence information onto the state of an ancilla. We successfully perform conversion of leakage errors via all major leakage pathways with a standard formulation of the LDU, benchmarking the performance of the LDU using a three-outcome low-loss state detection method. The LDU detects atom loss errors with  $\approx 93.4\%$  accuracy, limited by technical imperfections of our apparatus. We further propose, compile, and execute a SWAP LDU, wherein the roles of the original data atom and ancilla atom are exchanged under the action of the LDU, providing “free refilling” of atoms in the case of leakage errors. This circuit-based leakage-to-erasure error conversion is a critical component of a neutral atom quantum processor where the quantum information may significantly outlive the lifetime of any individual atom in the quantum register.

## I. INTRODUCTION

Neutral atoms have seen tremendous progress recently as a scalable platform for quantum computation [1–11]. The ease of scalability combined with parallel gate control and mid-circuit reconfigurability result in a platform with potential for fault tolerant quantum computation [12–14]. However, leakage out of the computational subspace is currently a substantial limitation in state-of-the-art systems [15] and remains a significant obstacle to the long-term prospects. Some degree of leakage is inevitable due to decay from the excited Rydberg state to other long-lived states. Another detrimental leakage channel that is specific to this platform is atom loss, which is expected in any sufficiently long quantum circuit due to the shallow trap depth. Transport of atoms mid-circuit for logic operations is also expected to result in increased atom temperature and atom loss. Leakage errors are difficult to correct in a fault tolerant way and generally require a significant overhead [16].

To deal with leakage errors, previous neutral-atom fault-tolerant protocols have employed hardware-specific methods [13, 17, 18] or circuit methods [12]. In alkaline-earth-like atom encodings, leakage pathways may be detected by leveraging their particular level structure, while keeping the qubit information intact [19, 20]. Detecting a leakage error converts it into an erasure error, which is easier to handle than generic unknown errors [13]. In the absence of such hardware-specific techniques, circuit-based methods known as Leakage Detection Units

(LDUs) may be used to detect leakage errors [21, 22]. LDUs map the information about whether or not a data atom is present and within the qubit subspace onto the 0/1 states of an ancilla atom without disturbing the information in the data atom in the case of no leakage. Similar circuit-based approaches to leakage errors have been previously demonstrated in other hardware such as trapped ions and superconducting qubits [23–27].

In this work, we study the application of LDUs for neutral atoms and perform proof-of-principle demonstrations of their implementation, demonstrating successful detection of leakage while preserving the coherence of the data qubit. The objectives of an LDU are twofold: 1) detect whether or not some data atom is in the computational subspace, and 2) do so in a way that preserves the information in that data atom. In this work, our qubit states are the “clock-state” Zeeman sublevels in the hyperfine ground-state manifold of cesium atoms in optical tweezers. For hyperfine ground state qubits in alkali atoms, there are three major pathways for the atom to leak out of the computational space (see Fig. 1). The first is atom loss from the trap due to background gas collisions, heating after many gates or movement operations, and atom drift when the traps are turned off during entangling operations. The second is Rydberg-leakage where population is unintentionally left behind in a short-lived Rydberg state after entangling operations, either due to coherent over-rotations or black-body induced transitions to nearby Rydberg states. The third leakage mechanism is so-called “hyperfine-leakage” into non-qubit Zeeman sublevels of the hyperfine ground manifold due to decay from excited states. Therefore, our objective is to demonstrate detection of leakage via these three pathways with a circuit that preserves the coherence of the data atom.

In Sec. II, we describe the major leakage pathways in

\* mnchow@sandia.gov

† bsdvikas@unm.edu

‡ These authors contributed equally to this work

detail and show how they can be accounted for and detected using LDUs. This is achieved by turning Rydberg leakage into atom loss via the repulsive force of the trap for population left behind in a Rydberg state (Rydberg anti-trapping) and by using two-qubit gates that are sensitive to the choice of Zeeman sublevel. We perform a proof-of-principle demonstration of the standard LDU, showing that the state of an ancilla atom correctly labels the presence or absence of a data atom within the qubit subspace without disturbing the information in the data atom. Then in Sec. III we discuss how this LDU can be modified for a neutral atom architecture to provide “free refilling” of atoms by performing a SWAP. We further implement a teleportation-based version of the SWAP LDU which has only one entangling gate and free refilling capability. These demonstrations are made possible by a three-outcome measurement protocol, which retains the atom in the trap after detection and can detect atom loss by direct measurement, allowing us to benchmark the performance of the LDUs [28, 29]. In the absence of the three-outcome measurement capability, the circuits presented here may still be used to mitigate leakage error, although in some cases work instead only as “Leakage Reduction Units” (LRUs) which reduce, but do not detect, leakage errors.

In addition to detecting leakage errors, we propose that the SWAP LDU provides a potential strategy for mid-circuit mitigation of atom heating and its resulting deleterious effects on atom loss and gate fidelity. For long circuits on this platform, heating of atoms will generally result from repeated applications of entangling gates (during which the optical tweezer trap is typically turned off and then atoms are recaptured) and from transport to rearrange the atomic configuration [30, 31]. As the SWAP LDU replaces a data atom with a “fresh” cold ancilla atom, it could be a powerful tool for maintaining a full, cold quantum register of data carriers by swapping in new atoms at a rate commensurate with atom loss and heating.

### A. Methods

The entangling gate we use throughout this work is a  $ZZ$  rotation by angle  $\theta$  via adiabatic Rydberg dressing [32]. In all cases, we echo the single-atom light shift as in Refs. [33, 34]. However, we use only the single-qubit  $\pi$ -pulse that performs the echo from that protocol, (dropping the outer  $\frac{\pi}{2}$ -pulses) so the three-pulse gate effectively performs the unitary  $R_{zz}(\theta)R_y(\pi)$ . The notation  $R_i(\theta)$  is used throughout this work to represent rotations about Bloch-sphere axis  $i \in \{x, y, z\}$  by angle  $\theta$  according to the unitary,  $\exp[-i\frac{\theta}{2}\hat{\sigma}_i]$ , where  $\hat{\sigma}_i$  is a Pauli operator.  $R_{zz}(\theta)$  is the two-qubit analog representing the unitary,  $\exp[-i\frac{\theta}{2}(\hat{\sigma}_z \otimes \hat{\sigma}_z)]$ . From Bell state fidelity measurements [35–38] after 1, 5, and 9 applications of  $R_{zz}(\frac{\pi}{2})R_y(\pi)$ , we estimate the two-qubit gate fidelity to be 0.967(+5, -7) (see Fig. 6) [39]. Globally-

addressed single-qubit  $R_\phi(\theta)$  rotations by angle  $\theta$  about equatorial axis  $\phi$  are driven with a Raman beam as in Ref. [40] with short-timescale (not accounting for hours-scale experiment drift) fidelity  $\approx 0.998(1)$  for a  $\pi$ -pulse, estimated from the ratio of the Rabi rate and exponential decay rate of the Rabi oscillations. Globally-addressed single-qubit  $R_z(\theta)$  gates are performed virtually via a phase advance of the local oscillator and are assumed to be error free.

Independent state detection of each atom is performed via a low-loss state detection (LLSD) technique [41] wherein the fluorescence from each trap site is coupled into an optical fiber and sent to a detector [28, 29]. Atoms are retained in the trap with high probability after state detection and we perform a second, state-insensitive detection stage to read out the final presence/absence of the atom in the trap. Therefore, LLSD is a three-outcome measurement revealing 0, 1, or ‘neither’ (no atom), and we typically postselect against the neither condition. The neither outcome is able to measure atom loss with high accuracy and is used as a benchmark to measure the performance of the LDUs in this work. The combined effects of state preparation and measurement (SPAM) errors and single-qubit gate errors from a  $\pi$  pulse result in a measured single-atom SPAM fidelity of 0.990(7). This  $\approx 1\%$  SPAM uncertainty applies to all following results reported in this work (reported numbers for LDU performance are not SPAM-corrected). Further details of the apparatus are described in previous work [29].

## II. STANDARD LDU WITH TWO ENTANGLING GATES

We use an LDU adapted from [12, 23, 25] and originally proposed in [21, 22], to non-destructively map a variety of leakage errors (including atom loss) in a data atom onto the state of an ancilla atom (see Fig. 2). This “standard” LDU, using the equivalent of two fully-entangling gates, is compiled to produce the identity on both the data ( $d$ ) and ancilla ( $a$ ) qubits ( $I_d I_a$ ) in the case that no leakage occurred and to produce a bit flip on the ancilla ( $X_a$ ) if leakage had occurred on the data atom prior to the LDU [42].

### A. Atom loss

Since atom loss is the most dominant leakage channel in our system and expected to be a critical challenge for neutral atom experiments at scale, we begin by testing the LDU performance in detecting the presence of the data atom in the trap. We test the performance of the LDU against atom loss errors by alternately preparing the data atom as being present or absent (in batches of 50). We directly verify the accuracy of the LDU against the final measurement of atom presence in the data atom site via LLSD. In the runs where LLSD reads out the

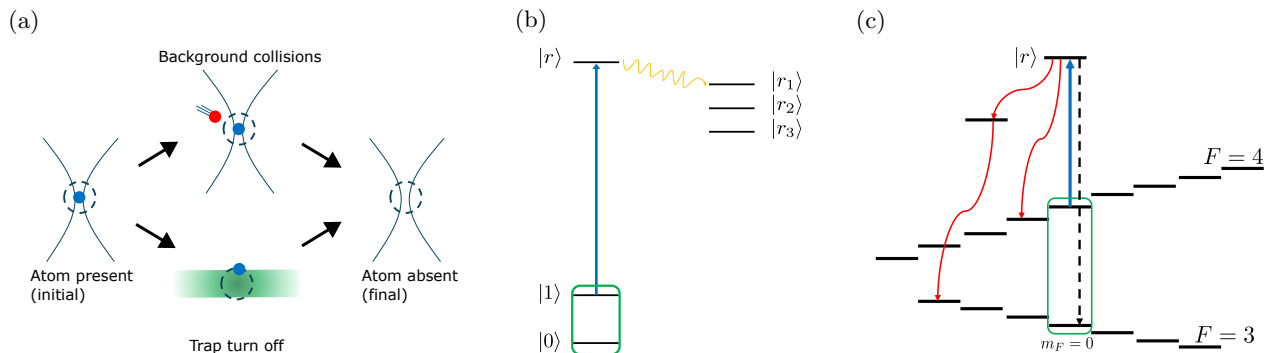


FIG. 1: There are three major leakage pathways for Rydberg atoms considered in this work. **(a)** Atom loss from the tweezer may occur due to background gas collisions (as illustrated in the top pathway of (a)), heating (not shown), or imperfect recapture efficiency (as illustrated in the bottom pathway of (a)) after turning off the trap during Rydberg laser (green shaded region) operation. **(b)** During entangling gates, population may be unintentionally left behind in the Rydberg state used for the gate ( $|r\rangle$ ) and may decay to other Rydberg states ( $|r_i\rangle$ ). This is called Rydberg leakage. **(c)** Both Rydberg population decay and off-resonant scattering from Raman or trap lasers can cause so-called “hyperfine leakage” (depicted as red curved arrows) into non-clock ground hyperfine sublevels, either directly or through intermediate excited states. Decay into the qubit subspace denoted by the green rectangle is not leakage, but instead falls under depolarizing or dephasing errors.

data atom as present, the state of the ancilla atom correctly identifies atom presence in  $765/814 \approx 94\%$  shots where the ancilla atom is also retained. When the data atom is absent, the ancilla atom correctly identifies it in  $919/984 \approx 93.4\%$  shots where the ancilla atom is retained. Inaccuracy of the LDU result when the data atom is present is dominated by gate errors (primarily two-qubit gates), whereas atom-absent inaccuracy is a combination of gate errors and finite probability of losing the data atom during or after the LDU. The measured atom-absent accuracy of the LDU is slightly better ( $865/901 \approx 96\%$  of shots) in the case that the atom is intentionally prepared as absent, indicating better performance when a given atom loss event is known to occur prior to the LDU (see A 2 for full raw data). As made possible by a three-outcome LLS, these results are post-selected for ancilla atom retention. Post-selection resulting in exclusion of a shot of the experiment due to loss of the ancilla occurred in  $202/2000 \approx 10\%$  of the total runs of the experiment.

We also demonstrate that the coherence of the data atom is preserved after the LDU through a Ramsey experiment with the LDU inserted; see Fig. 2c. Without the LDU, fitted contrast in the Ramsey experiment is  $99.9(+1, -7)\%$ , and with the LDU inserted, the contrast is  $95(1)\%$ . The contrast reduction is consistent with our single- and two-qubit gate fidelities. As the entangling gate infidelity is estimated at  $3.3(+7, -5)\%$  (see Fig. 6), the two entangling gates of the standard LDU constitute the majority of the error that leads to loss in contrast.

To confirm that the LDU is independent of input state of the data atom, we prepare the data atom in six different input states. This is accomplished by using the trapping beams to perform local  $\hat{\sigma}_z$  rotations via the differential light shift [43]. While these rotations are slow

(tens of  $\mu\text{s}$ ) and the fidelity of these operations is poor compared to the global single-qubit rotations, it is sufficient for the individual state preparation needed here. As our desired circuit begins with  $R_x(\frac{\pi}{2})$  on the ancilla atom and we wish to prepare various input states of the data atom,  $|\psi\rangle_d$ , we prepare the data atom along the  $x$ -,  $y$ -, or  $z$ -axis of the Bloch sphere without impacting the state of the ancilla by following an initial global  $R_x(\frac{\pi}{2})$  with a rotation by  $R_z(\xi)$  about the  $z$ -axis on just the data atom and then a rotation  $R_y(\theta)$  about the  $y$ -axis globally. Results for all six input states are given in Table I and confirm that the protocol is agnostic to the input state on the data atom.

## B. Rydberg leakage

Having demonstrated detection of atom presence with the standard LDU, we now turn to Rydberg state population leakage. Data atom population stuck in Rydberg states can still participate in entangling interactions with the ancilla (unlike atom loss) and lead to undesired outcomes for the LDUs. For example, if the data atom starts off in the Rydberg state used for the entangling gate,  $|r\rangle$ , during a CZ gate [32, 44], the ancilla atom ends up in  $|r\rangle$  with finite probability, propagating the leakage error [45]. This particular leakage does not satisfy the “sealed two-qubit gate” requirement [16] and can propagate during entangling interactions.

Since our Rydberg state ( $64P_{3/2}$ ) is anti-trapped for our trap wavelength (937 nm), Rydberg state population errors may be naturally converted to atom loss errors simply by turning on the trap. We measure the speed at which a Rydberg atom is ejected from the trap by promoting an atom to the Rydberg state with a  $\pi$ -pulse,

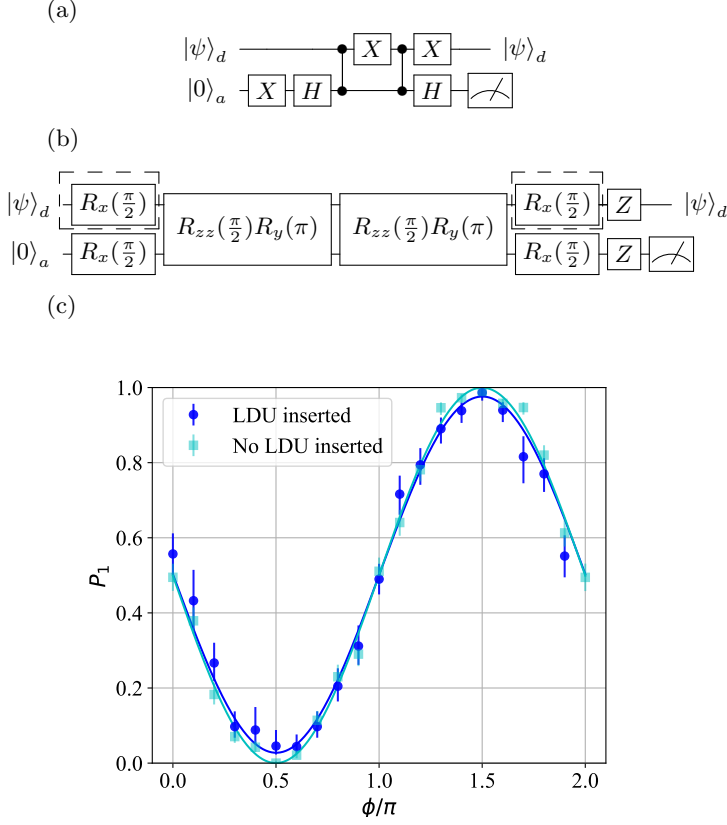


FIG. 2: ‘Standard’ leakage detection units (LDUs) using two entangling gates are composed to produce the identity on both the data (\$d\$) and ancilla (\$a\$) qubits (\$I\_d I\_a\$) in the case that no leakage occurred and produce a bit flip on the ancilla (\$X\_a\$) if leakage had occurred prior to the LDU. (a) The standard LDU composed of CZ, X, and H gates (typical native gates for neutral atoms) performs \$I\_d I\_a\$ in the case of no leakage and \$X\_a\$ in the case that the data atom has leaked out the qubit subspace (wherein CZ becomes an identity). (b) A standard LDU compiled for our native gates, using only globally-addressed single-qubit gates. The LDU implements \$I\_d I\_a\$ in the ideal case where no leakage has occurred and \$X\_a Z\_a\$ in the case where leakage has occurred. As a pair, the \$R\_x\$ pulses on the data atom (enclosed in dashed boxes) are optional, and do not change the logical operation. (c) A Ramsey coherence measurement on the data atom with (blue circles) and without (teal squares) insertion of the LDU as written in (b) demonstrates preservation of the quantum state of the data atom after the LDU. Probability of measuring the atom to be in the \$|1\rangle\$ state (\$P\_1\$) is shown as a function of the phase (\$\phi\$) of a final \$R\_\phi(\pi/2)\$ pulse. Uncertainty markers on datapoints are 68% Wilson score intervals.

\$ \psi\rangle_d\$	Atom present accuracy	Atom absent accuracy
-y	0.940(\$^{+7}_{-8}\$)	0.934(\$^{+7}_{-8}\$)
+y	0.94(1)	0.93(1)
+x	0.95(1)	0.92(1)
0	0.94(1)	0.95(1)
1	0.92(1)	0.94(1)
-x	0.93(1)	0.91(1)
Average	0.938(4)	0.931(4)

TABLE I: Standard leakage reduction unit performance with varied input state shows that the LDU works for all data atom input states. The accuracy of the LDU in labelling the data atom presence is verified by the state-independent detection stage of the LLSD. When the data atom is present (absent) as read out by the LLSD, the atom present (absent) accuracy displayed in column 2 (column 3) is assessed as the ratio of shots where the ancilla state after the LDU correctly labels the data atom presence over the total number of shots where the ancilla is retained. Uncertainties reported are 68% Wilson score intervals, reported symmetrically in cases where upper and lower intervals have the same most significant digit.

holding it for a variable amount of time, de-exciting it with a second \$\pi\$-pulse, and measuring the probability that the atom remains in the trap afterwards (see Fig. 5). In our system the survival drops by \$1/e\$ in \$\approx 23 \mu s\$, which is short compared to the Rydberg lifetime of \$\approx 170 \mu s\$ for the \$64P\$ state at room temperature [34, 46]. Trap wavelength, strength, geometry, and chosen Rydberg level all make the anti-trapping speed system-specific [47]. Once converted to atom loss, Rydberg state population errors are detectable with the LDU as before.

We note that with LLSD capability, atom loss errors (from Rydberg anti-trapping or otherwise) are typically postselected against. Postselection on atom retention has been used to improve effective entangling gate fidelity at the expense of postselection rate [48]. We also note that the entangling gate performance reported in this work similarly benefits from this form of postselection against atom loss (and therefore Rydberg leakage converted to loss by anti-trapping), but we leave an in-depth study of this contribution to future study.

### C. Hyperfine leakage

Finally, we test the performance of this LDU against leakage errors to other Zeeman levels in the ground state, i.e., hyperfine-leakage. We operate our experiment at 3.89 G bias magnetic field such that neighboring sub-levels in the ground (Rydberg) manifold are spectrally separated by 1.36 MHz (7.2 MHz). Therefore, neighboring sublevels are not expected to couple strongly to either the single- or two-qubit drive lasers and will be detectable as leakage errors via the LDU.

Our qubit computational basis states are the



$|F = 4, m_F = 0\rangle \equiv |1\rangle$  and  $|F = 3, m_F = 0\rangle \equiv |0\rangle$  states of the  $6S_{1/2}$  ground state manifold in Cs. By pulsing on an additional AOM-generated tweezer at a frequency separation equal to the Zeeman splitting (1.36 MHz), we are able to locally induce coupling between neighboring Zeeman levels in the ground state manifold via stimulated Raman transitions. Although the trapping light is nominally  $\pi$ -polarized, which should not permit transitions to  $\Delta m_F \neq 0$  states, the offset in position in the trapping plane and polarization vortices on the sides of the tightly-focused beams [49] provide sufficient polarization components to generate leakage to  $m_F \neq 0$  levels. Using a  $40\text{ }\mu\text{s}$  pulse of the additional tweezer, we drive leakage out of the qubit level with  $\approx 95.5\%$  ( $95.7\%$ ) probability after preparing in the  $|0\rangle$  ( $|1\rangle$ ) state. As the leakage-inducing pulse simply couples all neighboring Zeeman sublevels, the few percent remaining population in the clock state after the leakage pulse is expected.

When we use this post-leakage-inducing pulse state (which is a superposition of many  $m_F$  levels within one  $F$  manifold) as the data atom input state to the LDU, the ancilla reads out that the atom has leaked in  $371/415 \approx 89\%$  ( $355/407 \approx 87\%$ ) shots of the experiment when preparing in a mixture of  $F = 3$  ( $F = 4$ ) Zeeman sublevels. Ideally, the LDU would behave the same for non-qubit Zeeman sublevels as it would for an absent atom. For comparison, the atom-absent result was  $93.4\%$ . This difference between the atom loss and hyperfine leakage experiments is reasonably well-explained by the probability of remaining within the qubit subspace after the leakage-inducing pulse, implying similar leakage detection efficiency of this LDU for both hyperfine and atom loss leakage mechanisms. Any remaining discrepancy in performance, especially for the  $F = 4$  non-qubit states, could be due to weak, off-resonant coupling to the Rydberg state, and is left as a subject of further study which could be experimentally measured using shelving schemes [50].

Therefore, we have shown that all three major leakage pathways for alkali atoms (atom loss, Rydberg leakage, and hyperfine leakage) can be detected using the standard LDU, and that this LDU preserves the coherence of the data atom.

### III. SWAP LDUS

For neutral atom quantum computing architectures, there may be further advantages of LDUs that are compiled to perform a SWAP where the original data atom is replaced with a “fresh” reservoir atom in which the quantum information is now stored, and thus serves as the new data atom. As depicted in Fig. 3, these SWAP LDUs reduce the need for an extra refilling step after an LDU is performed, automatically supplying a re-initialized qubit in case of an atom loss. In addition, this could also allow for effective cooling of the data carriers by replacement of atoms. Heating incurred by, for example, repeated

entangling operations or non-adiabatic trap movements may then be effectively mitigated mid-circuit without disturbing the quantum information. In such a scheme, the fresh atoms would need to be swapped in sufficiently frequently to allow for high-fidelity operation of the entangling gates of the LDU before too much heat accumulates in any one atom. SWAP LDUs of this nature have the potential to be a powerful tool for reaching a paradigm where the quantum information for a calculation significantly outlives the physical lifetime of any single atom.

In the near term, such a regime may be reached by loading significantly more reservoir atoms than necessary for a computation [51] and replacing the data-carrier atoms continuously. For longer-term applications, recent progress on continuous atom reloading strategies suggests a way to continuously replenish atoms in a quantum register for indefinite operation [3, 52, 53].

These prospects assume that the atom loss probability increases as the data atom undergoes logic operations and that the ancilla atom presence probability is high after the LDU. While the SWAP LDU has the refilling advantages over the standard LDU, its failure rate increases with increasing ancilla atom loss rate before the LDU. Even a single failed round of LDU causes data information loss, since the original data atom is measured. In contrast, the standard LDU does not have this problem as the data atom is preserved at the end. Furthermore, using a three-outcome measurement, ancilla losses can be efficiently detected allowing their deleterious effects to be suppressed by postselection or subsequent attempts at the LDU. In state-of-the-art experiments, the ancilla loading fraction is expected to approach unity such that ancilla losses are expected to be a minor problem. As long as ancilla loss rate is small, this minor disadvantage of SWAP LDUs is expected to be far outweighed by the advantages of free refilling and cooling by replacement.

#### A. Teleportation-based LDU

In the SWAP LDU, we can combine the second entangling gate and the following measurement into a measurement feedback gate instead, as in a one-bit teleportation circuit [54, 55]. This circuit has previously been used as a “Leakage Reduction Unit” (LRU) that re-initializes a qubit into the computational subspace in the case of a leakage error, but cannot reveal if the leakage error occurred [55, 56]. In a quantum error correction setting, LRUs replace a leakage error with a Pauli error, which can then be corrected by further rounds of error correction.

We consider this same circuit but with a three-outcome measurement instead: a 0 outcome results in the conclusion that no local operation is needed and a 1 outcome results in a local Z operation to be applied on the new data atom for a successful SWAP. A “neither” measurement outcome reveals an atom loss, which has already been rectified with the new data atom carrying a  $|0\rangle$  state.

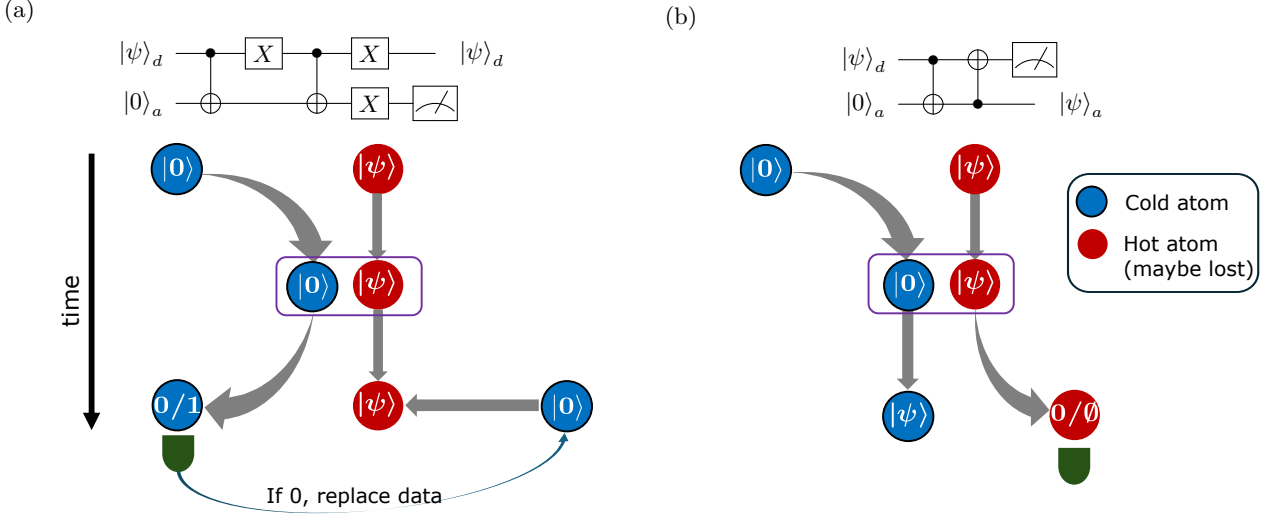


FIG. 3: Refilling advantages of SWAP LDUs. The data atom (red, no outline) carrying state  $|\psi\rangle$  is hot after going through many rounds of gates and rearrangement, and might have been lost or leaked. A fresh, cold ancilla atom (blue, dark outline) carrying  $|0\rangle$  is brought close to the data atom to apply an LDU. **(a)** In the standard LDU, the ancilla carries the information about the presence/absence of data atom and needs to be moved away for measurement. If the measurement gives 0, the data atom would need to be replaced with another fresh ancilla. **(b)** In the SWAP LDU, the LDU transfers the data  $|\psi\rangle$  onto the cold ancilla atom. The old data atom is borne away for a measurement. If the data atom was lost, it has already been replaced by the cold ancilla, removing the need for the extra refilling step. In addition, the data is always transferred onto a fresh cold atom. This kind of cooling by replacement may reduce potential problems from increasing atom temperature in operations later in the circuit.

Thus, a three-outcome measurement upgrades this LRU into an LDU, detecting leakage in addition to replacing it with a Pauli error. The main advantage of this “Z-teleportation” version of the LDU over the previously discussed circuit is that it requires only one entangling gate instead of two.

In a similar vein, our LLSD is not specific to the Zeeman-sublevel, so hyperfine leakage errors are not detected by this version of the LDU in our experiment. Given the long measurement times for neutral atoms, this LDU is likely to be useful instead of the SWAP LDU in cases where the conditional  $Z$  operator can be propagated into post-processing.

This LDU requires local single-qubit rotations, and as we do not currently have local measurement capabilities, we apply the measurement-controlled  $Z$  gate in post processing. We test the performance of this circuit and find that state  $|0\rangle$  is transferred correctly to the ancilla atom in  $597/624 = 95.7(8)\%$  of experiments and the state  $|1\rangle$  is transferred correctly in  $965/1007 = 95.8(7)\%$  of shots in which the data and ancilla atoms are retained. As a baseline, when no LDU is performed, the data qubit reads out correctly as  $|0\rangle$  in  $98.4(3)\%$  of shots and is read out correctly as  $|1\rangle$  in  $98.3(3)\%$  of experiments after state preparation using the local  $z$  rotations, implying that only 2-3% of the error stems from the LDU itself for the computational basis states.

Data atom loss errors are detected via LLSD in  $929/7150 \approx 13\%$  shots of the experiment (aggregating

all input states). In the case that the data atom is lost, we find that the remaining ancilla atom is measured to be in  $|0\rangle$  in  $396/794 \approx 50\%$  shots, consistent with initialization of the ancilla in  $| -x \rangle_a$  after the LDU in the case of detected leakage. We initialize in  $| -x \rangle_a$  instead of  $|0\rangle_a$  on the ancilla in the case of a leakage error because our circuit (Fig. 4b) differs from the teleportation LDU compiled with CZ and H (Fig. 4a) by a local rotation that does not impact the logical operation of the LDU.

More importantly, the original ancilla atom (new data atom) is similarly missing at the end of the computation in  $889/7150 \approx 12.4\%$  shots. Both atoms are lost in  $135/7150 \approx 1.9\%$  shots, consistent with independent random loss of the two atoms. While in this experiment, loss of the ancilla atom is mitigated by postselection on ancilla atom retention, (as made possible by LLSD) this loss reveals a fundamental limitation of the SWAP LDU atom replacement method. This effect is exaggerated here by a *technical* limitation of high atom loss rate, specific to our system. This fundamental limit is set by the combined loading accuracy of the ancilla atom and its retention probability after the LDU. For state-of-the-art experiments, loading accuracy approaches unity [1, 57] and loss probability after a single entangling gate can be suppressed to  $\leq 0.005$  [15].

To check the coherence of the quantum information after the teleportation-based LDU, we teleport a  $|+y\rangle$  and a  $| -x \rangle$  state and perform a phase scan of an effectively-local final  $R_\phi(\frac{\pi}{2})$  pulse to reveal the phase of the resulting

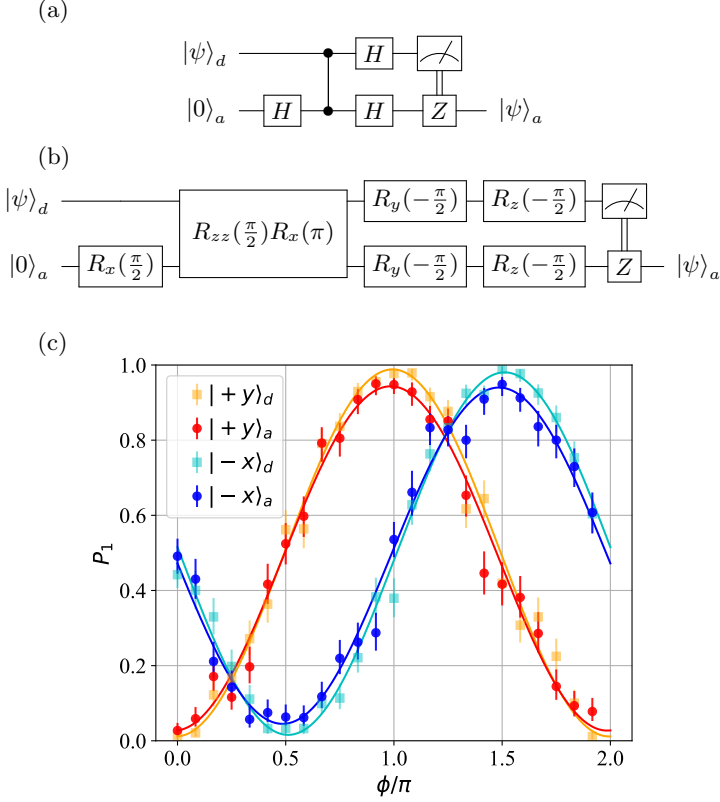


FIG. 4: Single-qubit teleportation LDU circuits compiled with typical gates (a) and our native gates (b). (c) Probability of measuring the  $|1\rangle$  state as the phase ( $\phi$ ) of a final  $R_\phi(\pi/2)$  pulse is scanned on the ancilla qubit (a) after teleportation of the  $|-x\rangle$  and  $|+y\rangle$  states (circles), with the same scan on the data qubit (d) with no LDU for reference (squares). Uncertainty markers on datapoints are 68% Wilson score intervals.

superposition state on the ancilla atom; see Fig. 4. As the physical local rotations can only perform  $R_z(\theta)$ , we split the global  $R_\phi(\pi/2)$  into two  $R_\phi(\pi/4)$  pulses and apply a local  $R_z(\pi)$  on the original data qubit in-between to effectively cancel its participation in the  $R_\phi$  gate [58]. [59] Compared to the direct data atom measurement in the case of no LDU, the contrast of the resulting teleported state is reduced from 96(1)% to 90(2)% for the  $|-x\rangle$  state and from 98(1)% to 92(2)% for the  $|+y\rangle$  state.

#### IV. DISCUSSION

The experiments in this work have demonstrated proof-of-principle detection of the three major leakage channels in neutral atom quantum computing platforms via LDUs, converting leakage errors into erasure errors. We also explored a SWAP LDU variation that could work well in a neutral atom architecture with potential refilling advantages. The majority of the errors in this work stem from the limited fidelity of entangling gates and lo-

cal addressing operations in our apparatus, which would be substantially better in state-of-the-art neutral atom systems [15, 51, 60].

The LDUs in this work are readily compiled using typical native gates of neutral atom systems (e.g., CZ, H, X, Z) and can be composed using globally-addressed single-qubit rotations (as in Fig. 7a), facilitating implementation on other experiments. Additionally, the standard LDUs used in this work were compiled for  $I_d I_a$  in the case of no leakage and  $X_a$  in the case of leakage simply for the convenience of circuit and result interpretation. The number of single-qubit gates may be reduced in some cases if we relax the requirements on the LDU to simply preserve the state information up to a local unitary and/or allow for flipped interpretation of the ancilla readout results. Similarly, hardware-optimized versions of these LDUs may be compiled to combine two entangling gates into a single gate of larger rotation angle to reduce the number of Rydberg laser pulses as in Fig. 7b.

We note that the three-outcome LLS technique made it possible to benchmark the performance of the LDUs in this work. In experiments where only two-outcome measurements are available, the standard LDU and the SWAP LDU can still be utilized, but would need an adjusted method of characterizing performance. By using a three-outcome measurement, the standard LDU can also detect ancilla loss, making it more robust. In a quantum error correction setting, replacing leaked qubits with qubits in the computational subspace is sufficient, as it can then be corrected during subsequent error correction rounds. In such a scenario, the teleportation LDU may also still be used as an LRU with two-outcome measurements, as it replaces a leaked qubit with a state in the qubit subspace. There may still be unexplored advantages for the three-outcome measurements for LDUs and other protocols involving mid-circuit measurements, which we leave as a subject of future study.

We also emphasize that the SWAP LDU is a promising approach to keeping a quantum register of atoms cold (and full) for long circuits without adding undue experimental burden. Similarly to sympathetic cooling in trapped ions [61], alternate approaches to cooling include sympathetic cooling of single neutral “impurity” atoms as used in BEC studies [62], although these approaches have not yet been shown to preserve coherence of a quantum register of atoms in tweezers and require laser cooling of an additional atomic species. Cooling atoms by scattering light in a coherence-preserving subspace is another proposed approach [17], but it requires additional level structure and control not readily available for alkali atoms. By contrast, the SWAP LDU is done by design with a single atomic species and only circuit-based control already required for a quantum processor. The only experimental overhead incurred is in the loading of additional atoms in the system, either by loading extra atoms before the circuit or continuously loading in a spatially-separated region [3]. This extra atom loading requirement is well within reach of current neutral

atom quantum processors, as repeated readout of a data atom using multiple ancillas (via extra atoms loaded before the circuit) has already been demonstrated in [51].

These proof-of-principle experiments demonstrate the potential benefits of LDUs for neutral atom quantum processors, though we did not comprehensively study the errors caused by the LDUs themselves and how they might propagate. Understanding the kind of errors that are produced by neutral atom entangling gates and how they affect the performance of individual LDUs is an important open question. Similarly, analysing how often LDUs or LRUs would need to be implemented during error correction rounds in a fault-tolerance setting for a neutral atom system is another significant task left to future work [16]. The fact that the LDU circuits presented here are essentially the same as LRUs that have been embedded in error correcting codes [26] shows great promise for the future implementation of the circuits studied here in such a fault-tolerant setting for neutral atoms.

## ACKNOWLEDGMENTS

We thank Anupam Mitra for helpful discussions and feedback during the drafting of this manuscript. We thank Roger Ding for helpful discussions about sympathetic cooling.

This work was supported by the Laboratory Directed Research and Development program at Sandia National Laboratories, a multimission laboratory managed and operated by National Technology and Engineering Solutions of Sandia LLC, a wholly owned subsidiary of Honeywell International Inc. for the U.S. Department of Energy's National Nuclear Security Administration under contract DE-NA0003525. This written work is authored by an employee of NTESS. The employee, not NTESS, owns the right, title and interest in and to the written work and is responsible for its contents. Any subjective views or opinions that might be expressed in the written work do not necessarily represent the views of the U.S. Government. The publisher acknowledges that the U.S. Government retains a non-exclusive, paid-up, irrevocable, world-wide license to publish or reproduce the published form of this written work or allow others to do so, for U.S. Government purposes. The DOE will provide public access to results of federally sponsored research in accordance with the DOE Public Access Plan. SAND2024-059040

## Appendix A: Supporting Data

### 1. Rydberg state anti-trapping measurement

Rydberg state anti-trapping speed measurement for the  $64P_{3/2}$  state of Cs in our tweezers is measured by promoting a single atom to the Rydberg state, holding it in the trap for a variable amount of time, de-exciting it, and measuring the probability that the atom is retained in the trap. See Fig. 5.

### 2. Full shot-by-shot data for standard LDU

For completion and clarity, we include a logic table with the results of the standard LDU experiment in Table II.

Additionally, we provide further details on the difference between atom loss identification accuracy of the standard LDU in the case of intentionally prepared absent atoms and accidentally lost atoms. When we analyze the atom absent case of the standard LDU in only the instances where the data atom was intentionally prepared as absent, we find that the ancilla correctly reports the data atom as absent in  $865/901 \approx 96\%$  of shots, slightly better than the aggregate result of  $919/984 \approx 93.4\%$ . This indicates that when the data atom is absent prior to the LDU, the resulting ancilla state accuracy is slightly better. On the other hand, the reduction in accuracy overall (from contribution of the accidental losses) is indicative of atom loss errors during or after the LDU, which could allow for unknown propagation of errors after the atom loss event. In the 83 cases where the data

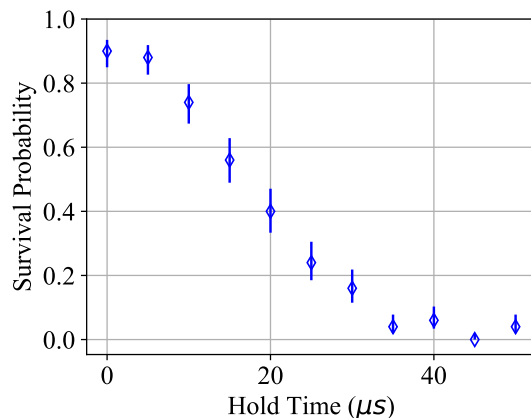


FIG. 5: Conversion of Rydberg state population errors to atom loss errors is done naturally by anti-trapping of atoms in the Rydberg state. Here we prepare the atom in the Rydberg state, hold the atom in the trap for a variable amount of time, and then de-excite the atom. Rydberg atoms are ejected from the trap after a few tens of  $\mu s$ . Uncertainty markers are 68% Wilson score intervals.



atom was initially loaded, but lost before the final read-out, the ancilla result reported the data atom as absent in 54 cases and present in 29 cases. These values are an indicator of when accidental atom loss is likely to occur in our system (before vs during or after the LDU).

Data atom	Ancilla atom	Result	N
0 or 1 (present)	0	Correct present	765
0 or 1 (present)	1	Incorrect absent	49
0 or 1 (present)	Neither (absent)	Postselect against	84
Neither (absent)	0	Incorrect present	919
Neither (absent)	1	Correct absent	65
Neither (absent)	Neither (absent)	Postselect against	118

TABLE II: Logic table and results for standard LDU experiment. In a total of 1000 shots of the experiment each, we attempt to prepare the data atom as present or absent (ancilla atom always intended to be present). For each shot, the LLSD outcome for the data atom (first column) and ancilla atom (second column) determine the our interpretation of the result (third column). Total number of shots for each outcome (N) are tabulated in the fourth column.

### 3. Bell state fidelity measurement for entangling gate

Data used in determining the two-qubit gate fidelity reported in this work is included in Fig. 6. We note that the fit to the parity oscillation uses Gaussian-distributed errors (Wald intervals), and may slightly overestimate contrast [51]. As discussed in the main text, these results include “natural” postselection against Rydberg leakage errors via anti-trapping and postselection against atom loss errors with LLSD. Fidelity ( $\mathcal{F}$ ) is assessed using population measurements and parity contrast according to [35–38]

$$\mathcal{F} = \frac{1}{2}(\rho_{00} + \rho_{11}) + \frac{1}{2}A, \quad (\text{A1})$$

where  $A$  is the fitted parity contrast and  $\rho_{ii}$  is the measured population in the  $|ii\rangle$  state.

### 4. Generic matrices for LDUs

Here we provide the process matrix for the standard LDU. The data atom may be in states  $\{0, 1, l\}$ , where  $|l\rangle$  represents leakage out of the qubit subspace. In the case that the data atom has not leaked, the LDU performs the identity, and in the case that the data atom has leaked, the LDU performs a bit flip on the ancilla. An unimportant phase ( $\phi$ ) may accompany the bit flip and has no logical consequence on the interpretation of the result.

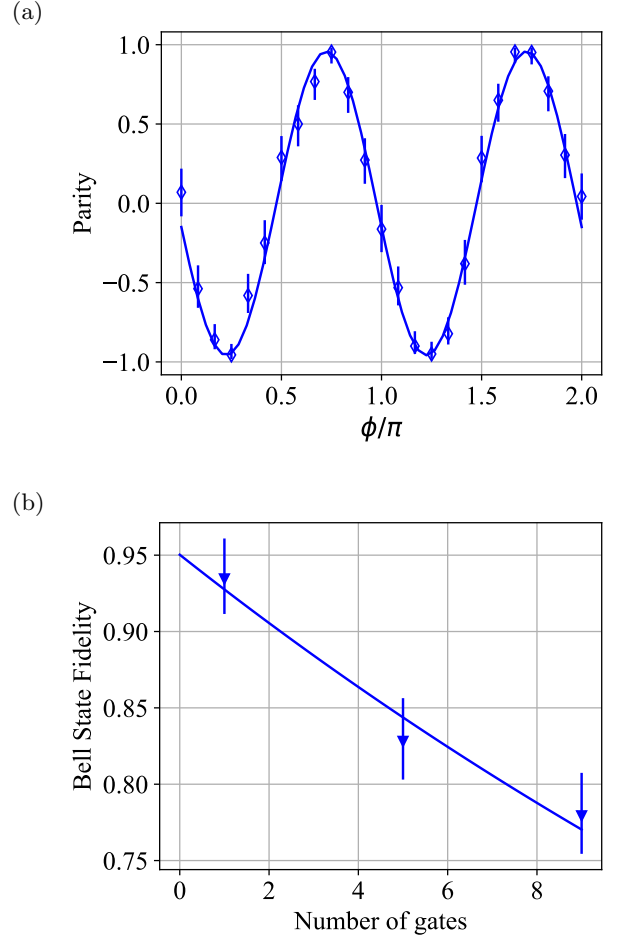


FIG. 6: Bell state fidelity measurement via parity scan of a final  $R_\phi(\frac{\pi}{2})$  pulse and population measurements for 1, 5, and 9 of the  $R_{zz}(\frac{\pi}{2})R_y(\pi)$  gate. **(a)** Parity scan example data for 1 entangling gate applied. Displayed errorbars are 68% Wilson score confidence intervals. **(b)** Fidelity as a function of the number of loops is fit to an exponential with a decay constant of 30(5) loops. Errorbars are derived from 68% Wilson score intervals on population measurements and fitting uncertainty on the parity contrast.

$$\begin{matrix} & \langle 00| & \langle 01| & \langle 10| & \langle 11| & \langle l0| & \langle l1| \\ \begin{matrix} |00\rangle \\ |01\rangle \\ |10\rangle \\ |11\rangle \\ |l0\rangle \\ |l1\rangle \end{matrix} & \begin{pmatrix} 1 & 0 & 0 & 0 & & \\ 0 & 1 & 0 & 0 & & \\ 0 & 0 & 1 & 0 & & \\ 0 & 0 & 0 & 1 & & \\ & & & & 0 & e^{i\phi} \\ & & & & e^{-i\phi} & 0 \end{pmatrix} \end{matrix} \quad (\text{A2})$$

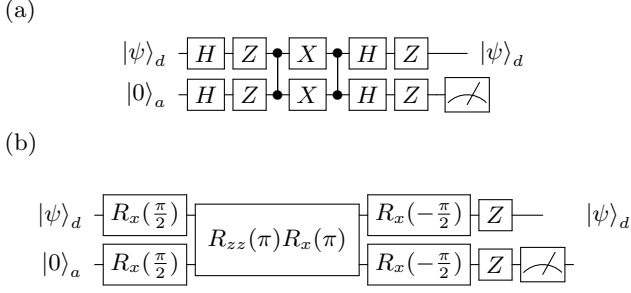


FIG. 7: Alternate versions of the LDUs. **(a)**

Global-addressing only version of the standard LDU, using gates native to typical neutral atom hardware.

**(b)** “Hardware optimized” version of the standard LDU that combines two fully-entangling  $R_{zz}(\frac{\pi}{2})R_\phi$  gates into a single  $R_{zz}(\pi)R_\phi$  gate to reduce the number of Rydberg laser pulses.

- 
- [1] D. Bluvstein, H. Levine, G. Semeghini, T. T. Wang, S. Ebadi, M. Kalinowski, A. Keesling, N. Maskara, H. Pichler, M. Greiner, V. Vuletić, and M. D. Lukin, *Nature* **604**, 451 (2022).
  - [2] H. J. Manetsch, G. Nomura, E. Bataille, K. H. Leung, X. Lv, and M. Endres, “A tweezer array with 6100 highly coherent atomic qubits,” (2024), [arXiv:2403.12021 \[quant-ph\]](#).
  - [3] M. A. Norcia, H. Kim, W. B. Cairncross, M. Stone, A. Ryou, M. Jaffe, M. O. Brown, K. Barnes, P. Battaglini, T. C. Bohdanowicz, A. Brown, K. Casella, C. A. Chen, R. Coxe, D. Crow, J. Epstein, C. Griger, E. Halperin, F. Hummel, A. M. W. Jones, J. M. Kindem, J. King, K. Kotru, J. Lauigan, M. Li, M. Lu, E. Megidish, J. Marjanovic, M. McDonald, T. Mittiga, J. A. Muniz, S. Narayanaswami, C. Nishiguchi, T. Paule, K. A. Pawlak, L. S. Peng, K. L. Pudenz, D. R. Perez, A. Smull, D. Stack, M. Urbanek, R. J. M. van de Veedonk, Z. Vendeiro, L. Wadleigh, T. Wilkason, T. Y. Wu, X. Xie, E. Zalus-Geller, X. Zhang, and B. J. Bloom, “Iterative assembly of  $^{171}\text{Yb}$  atom arrays in cavity-enhanced optical lattices,” (2024), [arXiv:2401.16177 \[quant-ph\]](#).
  - [4] S. Anand, C. E. Bradley, R. White, V. Ramesh, K. Singh, and H. Bernien, “A dual-species rydberg array,” (2024), [arXiv:2401.10325 \[quant-ph\]](#).
  - [5] B. Zhang, P. Peng, A. Paul, and J. D. Thompson, *Optica* **11**, 227 (2024).
  - [6] J. W. Lis, A. Senoo, W. F. McGrew, F. Rönchen, A. Jenkins, and A. M. Kaufman, *Phys. Rev. X* **13**, 041035 (2023).
  - [7] S. Ma, A. P. Burgers, G. Liu, J. Wilson, B. Zhang, and J. D. Thompson, *Physical Review X* **12** (2022), [10.1103/physrevx.12.021028](#).
  - [8] B. Nikolov, E. Diamond-Hitchcock, J. Bass, N. L. R. Spong, and J. D. Pritchard, *Phys. Rev. Lett.* **131**, 030602 (2023).
  - [9] L. Pause, L. Sturm, M. Mittenbühler, S. Amann, T. Preuschoff, D. Schäffner, M. Schlosser, and G. Birkel, *Optica* **11**, 222 (2024).
  - [10] A. Urech, I. H. A. Knottnerus, R. J. C. Spreeuw, and F. Schreck, *Phys. Rev. Res.* **4**, 023245 (2022).
  - [11] I. H. Deutsch, G. K. Brennen, and P. S. Jessen, *Fortschritte der Physik* **48**, 925–943 (2000).
  - [12] I. Cong, H. Levine, A. Keesling, D. Bluvstein, S.-T. Wang, and M. D. Lukin, *Phys. Rev. X* **12**, 021049 (2022).
  - [13] Y. Wu, S. Kolkowitz, S. Puri, and J. D. Thompson, *Nature communications* **13**, 4657 (2022).
  - [14] S. Omanakuttan, V. Buchemavari, J. A. Gross, I. H. Deutsch, and M. Marvian, “Fault-tolerant quantum computation using large spin cat-codes,” (2024), [arXiv:2401.04271 \[quant-ph\]](#).
  - [15] S. J. Evered, D. Bluvstein, M. Kalinowski, S. Ebadi, T. Manovitz, H. Zhou, S. H. Li, A. A. Geim, T. T. Wang, N. Maskara, H. Levine, G. Semeghini, M. Greiner, V. Vuletić, and M. D. Lukin, *Nature* **622**, 268 (2023).
  - [16] M. Suchara, A. W. Cross, and J. M. Gambetta, in *2015 IEEE International Symposium on Information Theory (ISIT)* (IEEE, 2015) pp. 1119–1123.
  - [17] S. Omanakuttan, V. Buchemavari, M. Martin, and I. H. Deutsch, in preparation.
  - [18] S. Omanakuttan, [arXiv preprint arXiv:2405.07885 \(2024\)](#).
  - [19] S. Ma, G. Liu, P. Peng, B. Zhang, S. Jandura, J. Claes, A. P. Burgers, G. Pupillo, S. Puri, and J. D. Thompson, *Nature* **622**, 279 (2023).
  - [20] P. Scholl, A. L. Shaw, R. B.-S. Tsai, R. Finkelstein, J. Choi, and M. Endres, *Nature* **622**, 273 (2023).
  - [21] J. Preskill, in *Introduction to quantum computation and information* (World Scientific, 1998) pp. 213–269.
  - [22] D. Gottesman, *Stabilizer codes and quantum error correction* (California Institute of Technology, 1997).
  - [23] S. A. Moses, C. H. Baldwin, M. S. Allman, R. Ancona, L. Ascarrunz, C. Barnes, J. Bartolotta, B. Bjork, P. Blanchard, M. Bohn, J. G. Bohnet, N. C. Brown, N. Q. Burdick, W. C. Burton, S. L. Campbell, J. P. Campora, C. Carron, J. Chambers, J. W. Chan, Y. H. Chen, A. Chernoguzov, E. Chertkov, J. Colina, J. P. Curtis, R. Daniel, M. DeCross, D. Deen, C. Delaney, J. M. Dreiling, C. T. Ertsgaard, J. Esposito, B. Estey, M. Fabrikant, C. Figgatt, C. Foltz, M. Foss-Feig, D. Fran-

- cois, J. P. Gaebler, T. M. Gatterman, C. N. Gilbreth, J. Giles, E. Glynn, A. Hall, A. M. Hankin, A. Hansen, D. Hayes, B. Higashi, I. M. Hoffman, B. Horning, J. J. Hout, R. Jacobs, J. Johansen, L. Jones, J. Karcz, T. Klein, P. Lauria, P. Lee, D. Liefer, S. T. Lu, D. Lucchetti, C. Lytle, A. Malm, M. Matheny, B. Mathewson, K. Mayer, D. B. Miller, M. Mills, B. Neyenhuis, L. Nugent, S. Olson, J. Parks, G. N. Price, Z. Price, M. Pugh, A. Ransford, A. P. Reed, C. Roman, M. Rowe, C. Ryan-Anderson, S. Sanders, J. Sedlacek, P. Shevchuk, P. Siegfried, T. Skripka, B. Spaun, R. T. Sprenkle, R. P. Stutz, M. Swallows, R. I. Tobey, A. Tran, T. Tran, E. Vogt, C. Volin, J. Walker, A. M. Zolot, and J. M. Pino, *Phys. Rev. X* **13**, 041052 (2023).
- [24] Z. Chen, J. Kelly, C. Quintana, R. Barends, B. Campbell, Y. Chen, B. Chiaro, A. Dunsworth, A. G. Fowler, E. Lucero, E. Jeffrey, A. Megrant, J. Mutus, M. Neeley, C. Neill, P. J. J. O'Malley, P. Roushan, D. Sank, A. Vainsencher, J. Wenner, T. C. White, A. N. Korotkov, and J. M. Martinis, *Phys. Rev. Lett.* **116**, 020501 (2016).
- [25] R. Stricker, D. Vodola, A. Erhard, L. Postler, M. Meth, M. Ringbauer, P. Schindler, T. Monz, M. Müller, and R. Blatt, *Nature* **585**, 207 (2020).
- [26] M. McEwen, D. Kafri, Z. Chen, J. Atalaya, K. J. Satzinger, C. Quintana, P. V. Klimov, D. Sank, C. Gidney, A. G. Fowler, F. Arute, K. Arya, B. Buckley, B. Burkett, N. Bushnell, B. Chiaro, R. Collins, S. Demura, A. Dunsworth, C. Erickson, B. Foxen, M. Giustina, T. Huang, S. Hong, E. Jeffrey, S. Kim, K. Kechedzhi, F. Kostitsa, P. Laptev, A. Megrant, X. Mi, J. Mutus, O. Naaman, M. Neeley, C. Neill, M. Niu, A. Paler, N. Redd, P. Roushan, T. C. White, J. Yao, P. Yeh, A. Zalcman, Y. Chen, V. N. Smelyanskiy, J. M. Martinis, H. Neven, J. Kelly, A. N. Korotkov, A. G. Petukhov, and R. Barends, *Nature Communications* **12**, 1761 (2021).
- [27] K. C. Miao, M. McEwen, J. Atalaya, D. Kafri, L. P. Pryadko, A. Bengtsson, A. Opremcak, K. J. Satzinger, Z. Chen, P. V. Klimov, C. Quintana, R. Acharya, K. Anderson, M. Ansmann, F. Arute, K. Arya, A. Asfaw, J. C. Bardin, A. Bourassa, J. Bovaird, L. Brill, B. B. Buckley, D. A. Buell, T. Burger, B. Burkett, N. Bushnell, J. Campero, B. Chiaro, R. Collins, P. Conner, A. L. Crook, B. Curtin, D. M. Debroy, S. Demura, A. Dunsworth, C. Erickson, R. Fatemi, V. S. Ferreira, L. F. Burgos, E. Forati, A. G. Fowler, B. Foxen, G. Garcia, W. Giang, C. Gidney, M. Giustina, R. Gosula, A. G. Dau, J. A. Gross, M. C. Hamilton, S. D. Harrington, P. Heu, J. Hilton, M. R. Hoffmann, S. Hong, T. Huang, A. Huff, J. Iveland, E. Jeffrey, Z. Jiang, C. Jones, J. Kelly, S. Kim, F. Kostitsa, J. M. Kreikebaum, D. Landhuis, P. Laptev, L. Laws, K. Lee, B. J. Lester, A. T. Lill, W. Liu, A. Locharla, E. Lucero, S. Martin, A. Megrant, X. Mi, S. Montazeri, A. Morvan, O. Naaman, M. Neeley, C. Neill, A. Nersisyan, M. Newman, J. H. Ng, A. Nguyen, M. Nguyen, R. Potter, C. Rocque, P. Roushan, K. Sankaragomathi, H. F. Schurkus, C. Schuster, M. J. Shearn, A. Shorter, N. Shutty, V. Shvarts, J. Skrzynny, W. C. Smith, G. Sterling, M. Szalay, D. Thor, A. Torres, T. White, B. W. K. Woo, Z. J. Yao, P. Yeh, J. Yoo, G. Young, A. Zalcman, N. Zhu, N. Zobrist, H. Neven, V. Smelyanskiy, A. Petukhov, A. N. Korotkov, D. Sank, and Y. Chen, *Nature Physics* **19**, 1780 (2023).
- [28] A. Fuhrmanek, R. Bourgain, Y. R. P. Sortais, and A. Browaeys, *Phys. Rev. Lett.* **106**, 133003 (2011).
- [29] M. N. H. Chow, B. J. Little, and Y.-Y. Jau, *Phys. Rev. A* **108**, 032407 (2023).
- [30] T. A. Savard, K. M. O'Hara, and J. E. Thomas, *Phys. Rev. A* **56**, R1095 (1997).
- [31] M. Schulz, *Tightly confined atoms in optical dipole traps*, Ph.D. thesis, University of Innsbruck (2002).
- [32] T. Keating, R. L. Cook, A. M. Hankin, Y.-Y. Jau, G. W. Biedermann, and I. H. Deutsch, *Phys. Rev. A* **91**, 012337 (2015).
- [33] A. Mitra, M. J. Martin, G. W. Biedermann, A. M. Marino, P. M. Poggi, and I. H. Deutsch, *Phys. Rev. A* **101**, 030301 (2020).
- [34] M. J. Martin, Y.-Y. Jau, J. Lee, A. Mitra, I. H. Deutsch, and G. W. Biedermann, "A mølmer-sørensen gate with rydberg-dressed atoms," (2021), [arXiv:2111.14677](https://arxiv.org/abs/2111.14677) [quant-ph].
- [35] C. A. Sackett, D. Kielpinski, B. E. King, C. Langer, V. Meyer, C. J. Myatt, M. Rowe, Q. A. Turchette, W. M. Itano, D. J. Wineland, and C. Monroe, *Nature* **404**, 256 (2000).
- [36] K. Kim, M.-S. Chang, R. Islam, S. Korenblit, L.-M. Duan, and C. Monroe, *Phys. Rev. Lett.* **103**, 120502 (2009).
- [37] T. A. Manning, *Quantum Information Processing with Trapped Ion Chains*, Ph.D. thesis, University of Maryland, College Park (2014).
- [38] C. Figgatt, A. Ostrander, N. M. Linke, K. A. Landsman, D. Zhu, D. Maslov, and C. Monroe, *Nature* **572**, 368 (2019).
- [39] For the spin echo of the entangling gate, we often choose to use a  $\pi$ -pulse about the  $y$ -axis to provide robustness to single-qubit pulse area errors when combined with preceding  $x$ -axis pulses [63].
- [40] H. Levine, D. Bluvstein, A. Keesling, T. T. Wang, S. Ebadi, G. Semeghini, A. Omran, M. Greiner, V. Vuletić, and M. D. Lukin, *Phys. Rev. A* **105**, 032618 (2022).
- [41] Sometimes LLSD is referred to as non-destructive readout (NDRO) in literature. We use LLSD to avoid confusion over the term "non-destructive", which could accidentally imply non-projective measurements. LLSD is a projective measurement of both the atom state and the atom presence in the trap.
- [42] Alternate compilations of LDUs may instead choose to perform the opposite logic and flip the interpretation of the readout result on the ancilla. We consistently use identity for no leakage and bit flip on the ancilla for convenience.
- [43] S. Kuhr, W. Alt, D. Schrader, I. Dotsenko, Y. Miroshnychenko, A. Rauschenbeutel, and D. Meschede, *Phys. Rev. A* **72**, 023406 (2005).
- [44] H. Levine, A. Keesling, G. Semeghini, A. Omran, T. T. Wang, S. Ebadi, H. Bernien, M. Greiner, V. Vuletić, H. Pichler, and M. D. Lukin, *Phys. Rev. Lett.* **123**, 170503 (2019).
- [45] For LP gate and the Adiabatic gate, if the two-atom initial state is  $|r1\rangle$ , the end state will be  $\approx \sqrt{0.7}|r1\rangle + \sqrt{0.3}|1r\rangle$ . If the initial state is  $|r_11\rangle$ , where  $|r_1\rangle$  is a different nearby Rydberg state, due to Black body radiation, then a coherent phase error is instead added on the second atom.

- [46] S. de Léséleuc, D. Barredo, V. Lienhard, A. Browaeys, and T. Lahaye, *Phys. Rev. A* **97**, 053803 (2018).
- [47] R. J. P. T. de Keijzer, O. Tse, and S. J. J. M. F. Kokkelmans, *Physical Review A* **108** (2023), 10.1103/physreva.108.023122.
- [48] T. Noel, VP for Quantum Computing, Inflection (private communication).
- [49] J. D. Thompson, T. G. Tiecke, A. S. Zibrov, V. Vuletić, and M. D. Lukin, *Phys. Rev. Lett.* **110**, 133001 (2013).
- [50] T. M. Graham, L. Phuttitarn, R. Chinnarasu, Y. Song, C. Poole, K. Jooya, J. Scott, A. Scott, P. Eichler, and M. Saffman, *Phys. Rev. X* **13**, 041051 (2023).
- [51] R. Finkelstein, R. B.-S. Tsai, X. Sun, P. Scholl, S. Dirckci, T. Gefen, J. Choi, A. L. Shaw, and M. Endres, “Universal quantum operations and ancilla-based readout for tweezer clocks,” (2024), [arXiv:2402.16220 \[quant-ph\]](https://arxiv.org/abs/2402.16220).
- [52] K. Singh, S. Anand, A. Pocklington, J. T. Kemp, and H. Bernien, *Phys. Rev. X* **12**, 011040 (2022).
- [53] C.-C. Chen, S. Bennetts, and F. Schreck, in *Advances in Atomic, Molecular, and Optical Physics*, Advances In Atomic, Molecular, and Optical Physics, Vol. 72, edited by L. F. DiMauro, H. Perrin, and S. F. Yelin (Academic Press, 2023) pp. 361–430.
- [54] X. Zhou, D. W. Leung, and I. L. Chuang, *Phys. Rev. A* **62**, 052316 (2000).
- [55] A. G. Fowler, *Phys. Rev. A* **88**, 042308 (2013).
- [56] P. Aliferis and B. M. Terhal, *Quantum Info. Comput.* **7**, 139–156 (2007).
- [57] A. L. Shaw, Z. Chen, J. Choi, D. K. Mark, P. Scholl, R. Finkelstein, A. Elben, S. Choi, and M. Endres, *Nature* **628**, 71 (2024).
- [58] A. L. Shaw, R. Finkelstein, R. B.-S. Tsai, P. Scholl, T. H. Yoon, J. Choi, and M. Endres, *Nature Physics* **20**, 195 (2024).
- [59] Note that a final, local  $R_z(\pi)$  pulse is generally needed, but omitted here as it is followed by a measurement.
- [60] A. Cao, W. J. Eckner, T. L. Yelin, A. W. Young, S. Jandura, L. Yan, K. Kim, G. Pupillo, J. Ye, N. D. Oppong, and A. M. Kaufman, “Multi-qubit gates and ‘schrödinger cat’ states in an optical clock,” (2024), [arXiv:2402.16289 \[quant-ph\]](https://arxiv.org/abs/2402.16289).
- [61] M. D. Barrett, B. DeMarco, T. Schaetz, V. Meyer, D. Leibfried, J. Britton, J. Chiaverini, W. M. Itano, B. Jelenković, J. D. Jost, C. Langer, T. Rosenband, and D. J. Wineland, *Phys. Rev. A* **68**, 042302 (2003).
- [62] N. Spethmann, F. Kindermann, S. John, C. Weber, D. Meschede, and A. Widera, *Phys. Rev. Lett.* **109**, 235301 (2012).
- [63] S. Meiboom and D. Gill, *Review of Scientific Instruments* **29**, 688 (1958), [https://pubs.aip.org/aip/rsi/article-pdf/29/8/688/19287064/688.1\\_online.pdf](https://pubs.aip.org/aip/rsi/article-pdf/29/8/688/19287064/688.1_online.pdf).